HELIOTEK
A Division of Textron Inc.
12500 GLADSTONE AVE., SYLMAR, CALIFORNIA 91342 · TWX 910-496-1488 · Area Code 213/365-6301

Development of an Integrated Lightweight Flexible Silicon Solar Cell Array

Quarterly Technical Report No. 1

July 1, 1969 to October 1, 1969

Prepared for:

Jet Propulsion Laboratory
California Institute of Technology
4800 Oak Grove Drive
Pasadena, California

Prepared under

Contract No. 952560

by

Heliotek, Division of Textron, Inc.
12500 Gladstone Avenue
Sylmar, California 91342

Development of an Integrated Lightweight Flexible Silicon Solar Cell Array

Quarterly Technical Report No. 1

July 1, 1969 to October 1, 1969

JPL Contract No. 952560

This work was performed for the Jet Propulsion Laboratory, California Institute of Technology, as sponsored by the National Aeronautics and Space Administration under Contract NAS7-100.

Prepared by

E. L. Ralph
E. F. Zimmerman
P. M. Stella

Heliotek, Division of Textron, Inc.
12500 Gladstone Avenue
Sylmar, California 91342

Table of Contents

List of Figures

ABSTRACT

This is the first quarterly report for the Development of an Integrated Lightweight Flexible Silicon Solar Cell Array. The study is to provide design data that will help in the development of lightweight flexible solar arrays which are significantly lighter and less expensive than arrays presently being designed. Included in this report are solar cell cost effectiveness comparison, a preliminary analysis of a continuous process solar cell ultra-thin cover installation process, a detailed analysis of solar cell interconnect stresses and an analysis of a ribbon substrate with associated test data.

SUMMARY

The object of this program is to analyze, develop and test the various components and systems which can be integrated to form a lightweight flexible solar cell array capable of producing 100 watts per pound at a price of $100 per watt. To achieve the objectives of this program the array study has been broken down into four tasks which are directly associated with the various components of the array. A literature search and review was performed to determine the current state-of-the-art development of lightweight arrays to minimize duplication of effort and to clarify the approach to be taken.

A survey was made to gain information on solar cell prices as a function of size, thickness, quantity and configuration.

In order to obtain useful cell price information, an analysis was conducted based upon cell prices from 1958 through 1969 along with some current data. A learning curve type trend became apparent and by utilizing this information, estimated cell prices for the present and a future (1974) period were generated. This allowed a comprehensive determination to be made of power (weight) cost versus cell thickness and an optimum cost effective cell design was identified. The optimum system presently available was found to utilize 8 mil thick cells. By 1974 it is estimated that 4 mil solar cells will become optimum. A preliminary analysis of a continuous ribbon glass cell cover process has been completed. The analysis was divided into two parts, adhesive selection and ribbon glass selection and sizing. Several adhesives were tested however. Sylgard 182 or Dow Corning XR6-3489 was determined the most satisfactory adhesive. A thin Corning 8871 high lead content ribbon glass was evaluated and methods of applying the glass to the cell were developed. It was determined that the ribbon configuration could be supplied in various chemical compositions including 0211 microsheet which is presently used for silicon solar cell covers thus minimizing the need for a comprehensive radiation evaluation

program. The availability of this composition glass adds great impetus to the study because of the opportunity to use a material with known properties.

The problems associated with handling and cutting glass 0.0013 inches thick were difficult and required special techniques for their solution. The approach followed was to bond the thin glass to the solar cell and trim the glass to size after the adhesive had cured. Three methods of trimming the glass were evaluated. They were a hot nichrome wire, a small precision sandblasting unit and a diamond scribe. A large number of samples were prepared and were trimmed using the various techniques. This evaluation resulted in acceptable trimmed edges with 51% of the diamond scribed covers, 44% for the sandblasted edges and 16% for the hot wire method.

An analysis of interconnector in design parameters was made. This analysis considered stress distributions, thermal cycling fatigue and vibrational fatigue. For a flexible lightweight array, the stress loop type interconnector was found to be a marginal design in respect to fatigue resistance. Consequently alternate interconnector concepts were investigated. A wrap-around type thin film interconnector was considered and appeared desirable for the lightweight array. An analysis of the lightweight ribbon substrate showed that bond strength was essentially independent of bond area or ribbon width. This allows one to design a substrate using narrow ribbons rather than completely covering the back of cells, thus saving considerable weight. This system not only eliminates the unnecessary film, but also eliminates much cell bonding adhesive that does not contribute to the structural integrity of the solar cell array. The analysis was begun by investigating the failure mechanism of the ribbon substrate concept. Results of the analysis indicated that up to a point the tensile strength of cells bonded in series using a polyimide ribbon and RTV silicon rubber was independent of the distance that the polyimide ribbon overlapped the cell. Optimum overlap was about 0.100 inches. This was based on the results of

tests conducted on 100 samples with film overlap of 0.050", 0.100", 0.150", 0.200" and 0.250".

1.0 INTRODUCTION

Solar cell development has progressed at a rapid rate for the past eight years and the units of merit, such as watts per pound and dollar per watt for individual solar cells have been significantly improved.

Unfortunately these improvements in all characteristics, although significant when applied to the individual cell weight and costs, do not have the same impact on the complete solar cell array. State-of-the-art array fabrication designs and techniques result in an array weight about ten times the weight of the essential active device, and result in costs that are increased by more than a factor of two. Obviously, if progress is to be made in the reduction of weight and cost of silicon solar cell arrays, it must include studies of all components in the array and not be restricted toward the solar cell device alone. As a result new materials and techniques are being investigated to determine the proper approach for making a significant improvement in array design. New array concepts along with unique fabrication methods are being studied, with the goals being increased power to weight ratios and a decrease in the cost per watt of power generated.

This report describes the progress of a program to develop an advanced concept integrated lightweight flexible solar cell array with inherent versatility. This array concept could be readily adapted to specific deployment designs and mission requirements. The ultimate goal of a flexible integrated array program such as this being proposed would be the development of processes to produce a solar cell array (complete with power bus, but excluding deployment mechanism) capable of producing 120 watts per pound at power levels greater than one kilowatt at a cost of approximately $100 per watt.

2.0 TECHNICAL DISCUSSION

The Heliotek integrated flexible solar cell array concept has evolved from an analysis of the cost and weight contributions made by each component or process in a typical complete array. The weight and cost contributions made by each component were then compared so that the areas where major improvements could be made were identified. New ideas for improved materials and methods were then applied to the various components to improve the design in respect to both superior performance and more economical manufacturing possibilities. The following sections discuss each component or area of study and illustrate ideas and concepts for utilizing more advanced technology or improving existing component performance. The net result anticipated from this development study, will be an improved overall solar cell array which will be versatile, and can be applied to all solar power systems. The ultimate objective in this study will be an advanced array made up of an integrated module of silicon solar cells about one foot square or larger which can be readily interconnected at low cost to make up a larger system. All critical operations such as cell contacting and coverglass application will be accomplished at this modular stage, so that only insensitive bus connections need to be made by the power systems facilities. This eliminates the need for many facilities to learn to work with highly critical operations such as cell contacting, which has proven to be quite variable from one facility to another with a reliability variability associated with it. In this design being developed a large integrated array of cells would be completely interconnected electrically and mechanically with a suitable flexible structural skin. This array would have integral metal bus members for power distribution. The application of this integrated array would be highly versatile. A large flexible array would be accomplished by simply bonding the integrated arrays together and interconnecting the metal bus members as desired. This large array could then be supported by any flexible deployment mechanism presently contemplated. The design also can be

conveniently applied to advanced rigid deployment systems such as the beryllium frame panel or conventional aluminum skin rigid panels, if the advantages of eliminating the substrate weight are not desired for a particular mission.

The following sections describe the work being performed to analytically evaluate the design factors that need to be optimized and the experimental work which has been done to evaluate new materials and process techniques.

2.1 SOLAR CELL EVALUATION AND SELECTION

The intent of the cell evaluation part of the lightweight array study was to determine the optimum cell configuration which would provide the best power to weight ratio at the least cost. Ideally a trade-off study such as this should be easily obtained by comparing costs of various size and thickness solar cells and relating this to the power output values. Actually this is not so simple since there are many cell types available and the number of variables becomes very large. Also the cell costs are highly dependent upon the degree of development of a particular cell type. In spite of these problems, an attempt was made to develop a matrix of cell types, and current costs were requested. The following variables were considered important for this program and were included in the matrix.

1. Standard bar cells - 2 x 2 cm
2. Wrap-around contact cells - 2 x 2 cm
3. Large area cells - 2 x 4 cm, 2 x 6 cm
4. Various cell thicknesses: 12, 8, 6, and 4 mils
5. Cell quantities from 10K to 2M.

This request for power output and general cost information resulted in either no information submitted or at best only partial answers to selected portions of the variable matrix. Analyzing the few data points thus available it became apparent that it would be impossible to gain any relevant trade-off information this way.

It was therefore decided that if current cost and performance data was not readily available, then maybe the trade-off design study could still be performed if the principles of cell economics could be defined. In order to define these principles a study was made of the solar cell field over the past years so as to determine what kinds of trends might be noticed. If definite trends were found then it was felt that extrapolations could be made to the present and future regarding such variables as new cell design acceptance, cell costs, performance and time factors.

In regard to solar cell costs it was concluded that at any particular time in history, the thinner the cell the higher the cost. Actually there normally was a range of cell thicknesses which were available at essentially the same price then as the thickness was decreased below this minimum (or conventional) thickness the price increased at a very rapid rate. Figure 2.1-1 shows this relationship over a fairly long period of time. Although these are basically schematic curves, there are usually one or two historical points on each curve that generally fixed the shape and magnitude of the curve. The curve was normalized to 1.0 for the thickest (least expensive) cell for any period of time so that only thickness effects were analyzed and general cost variations due to cell design, production efficiency, time period, size, etc., were put on an equal basis.

The value-one represents basically the state-of-the-art large volume production cell for that period of time. The first obvious fact that is evident is that the trend is to provide thinner solar cells as time goes on. Also the critical point where thinner cells cost appreciably more changes to thinner cells with time. Since these curves are continually changing, information today will not be satisfactory for projecting cost effective designs for future array designs. Therefore, for example, a curve is shown for a 1974 projected estimate that can be used in this study for making a cost effective array design. This 1974 curve is expected to be similar to the general patterns seen in the past, but will be shifted so that the critical break occurs between 4 and 6 mils cell thickness.

The reason for using this type of price relation is due to the fact that actual cell prices will be a function of many variables in addition to cell thickness. Therefore, since actual project requirements may vary, it was desirable to eliminate the effects of non-thickness related variables for this present analysis. Since thickness is the primary variable that affects the power to weight ratio, this is the variable that becomes critical for this lightweight array study.

Another characteristic cost curve that was observed was associated with a cell design change and the learning curve associated with the change.

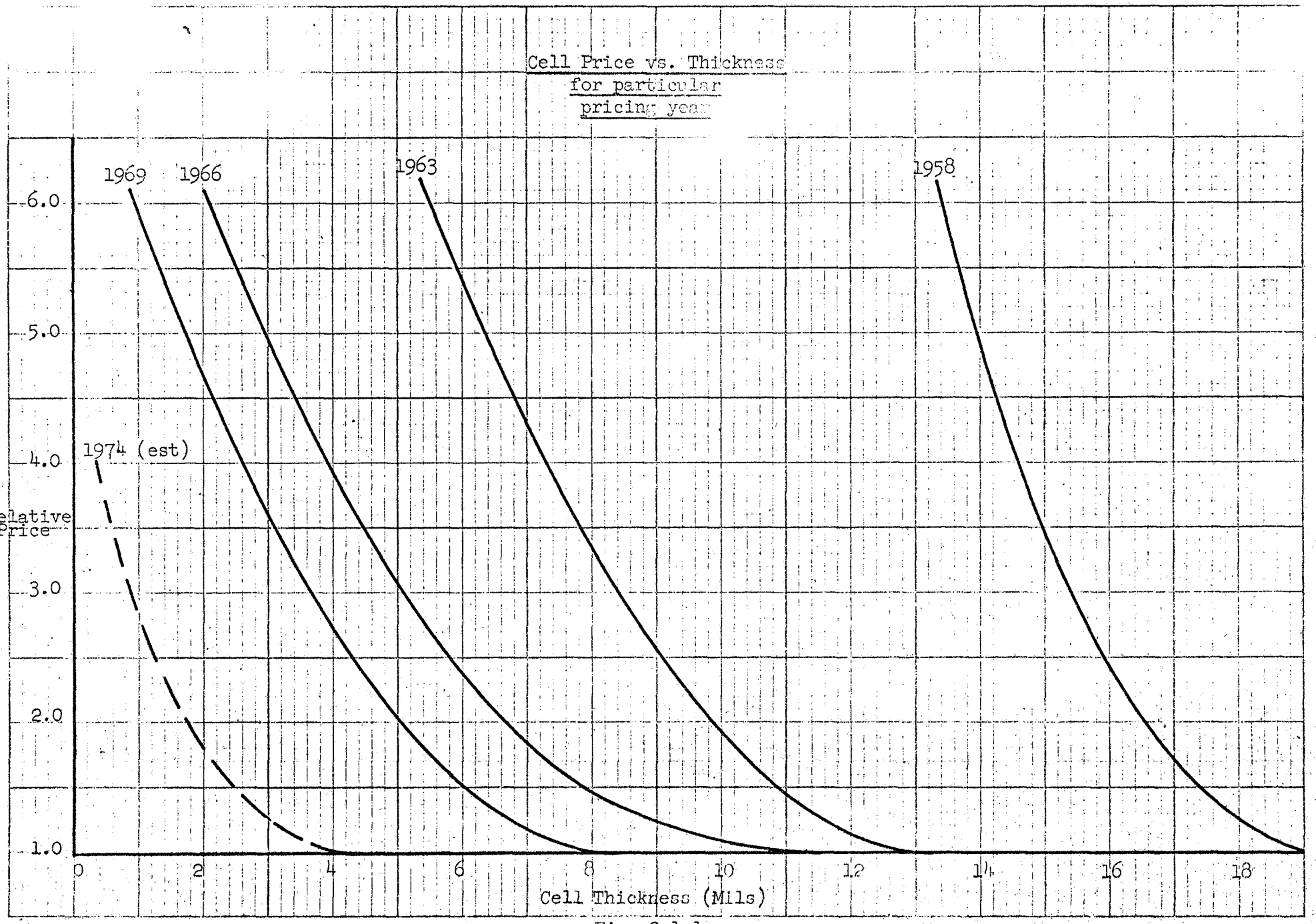
Cell Price vs. Thickness
for particular
pricing year
1969
1966
1963
1958
1974 (est)
6.0
5.0
4.0
3.0
2.0
1.0
Relative Price
0
2
4
6
8
10
12
14
16
18
Cell Thickness (Mils)

Fig. 2.1-1

Several significant historical design changes have taken place and can be used as examples. For instance, the change from P/N to N/P cells, the change from N contacts to titanium-silver contacts, the use of thinner cells, and the use of larger area cells. All of these examples had learning curve characteristics associated with the change that reflected in the cell costs. In all cases the initial change resulted in higher costs with a subsequent drop to a base level that was usually close to the initial base level. Some types of changes make a quick recovery, while other changes are more severe and require much time to reach the base level. Figure 2.1-2 shows schematically how these cell design changes typically appear in a cost analysis. N/P cells had a significant cost impact at first, but soon reached P/N cost levels. The 8 mil thick cells also had a significant cost impact, but were much slower to approach the thicker cell base line. The large area cells are an example where only a small cost impact was initially seen, then the learning curve was rapid and the costs dropped below the original base line level. The wrap-around cells are presently following a very slow learning curve; however this may be due to lack of interest or due to basic cost factors. In any case it is apparent that future cell design changes such as wrap-around design will follow these basic cost patterns and they must be characterized and predicted for any new cell design utilized in a cost analysis of new arrays. If these new cell design cost considerations are combined with the thickness effects we get a curve such as that shown in Figure 2.1-3. Both large area cells and wrap-around cells are of interest for this lightweight array study and are shown in this figure. In this plot the 1974 projected values show that the thin large area cells are more expensive than the thin 2 x 2 m cells while the thicker large area cells are less expensive. The wrap-around cells are shown to be more expensive than both other cell types in 1974 although this picture is likely to change if an extensive effort were placed on developing this type of cell.

If the results of the data in Figure 2.1-3 are incorporated with the cell performance data[1] for each type of cell, the outcome of this analysis is exhibited in Figure 2.1-4. This figure shows the relative power/

1) Performance of Very Thin Silicon Solar Cells, E. L. Ralph, Sixth Photovoltaic Specialists Conference, Cocoa Beach, Florida, March 1967

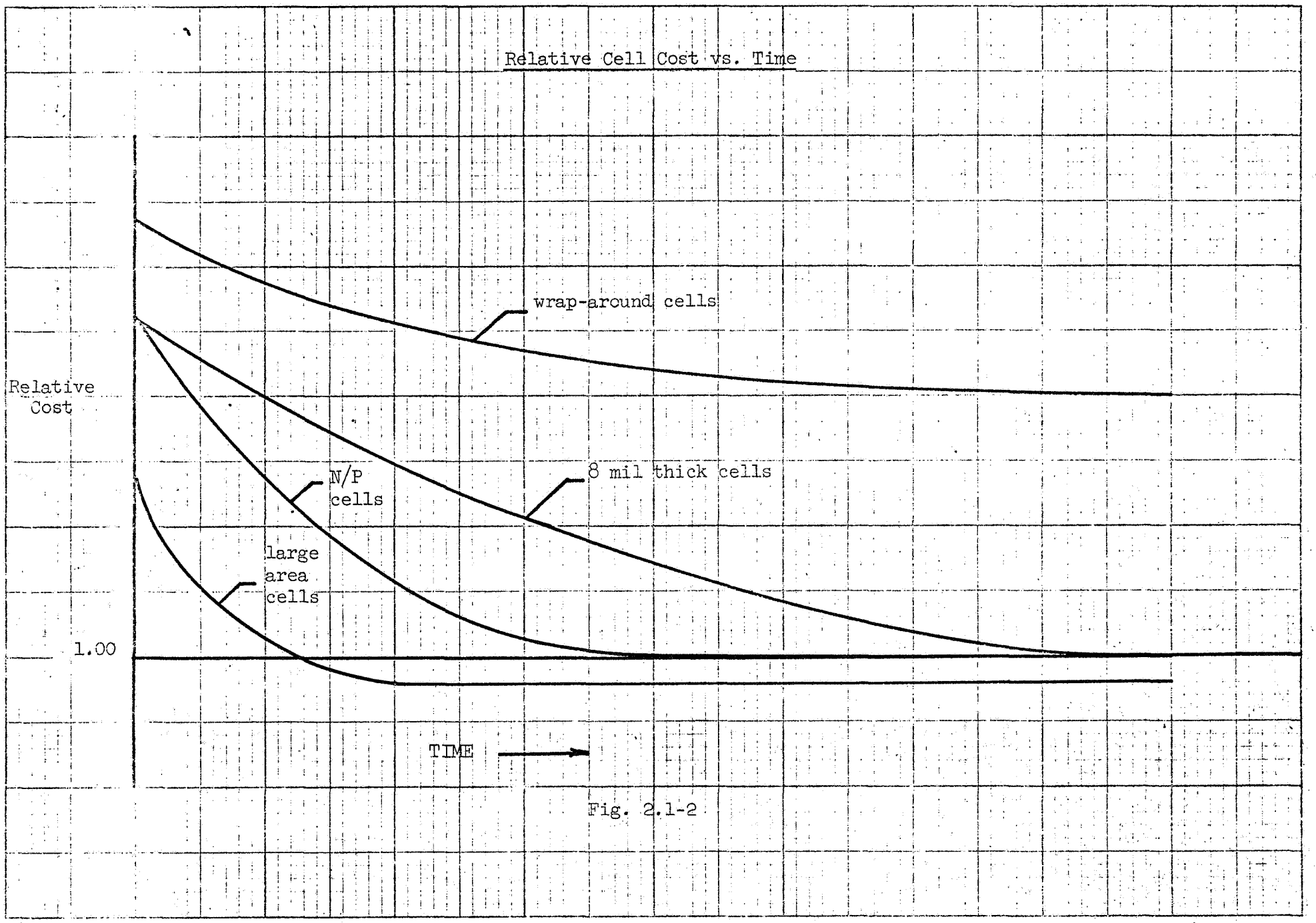

Fig. 2.1-2

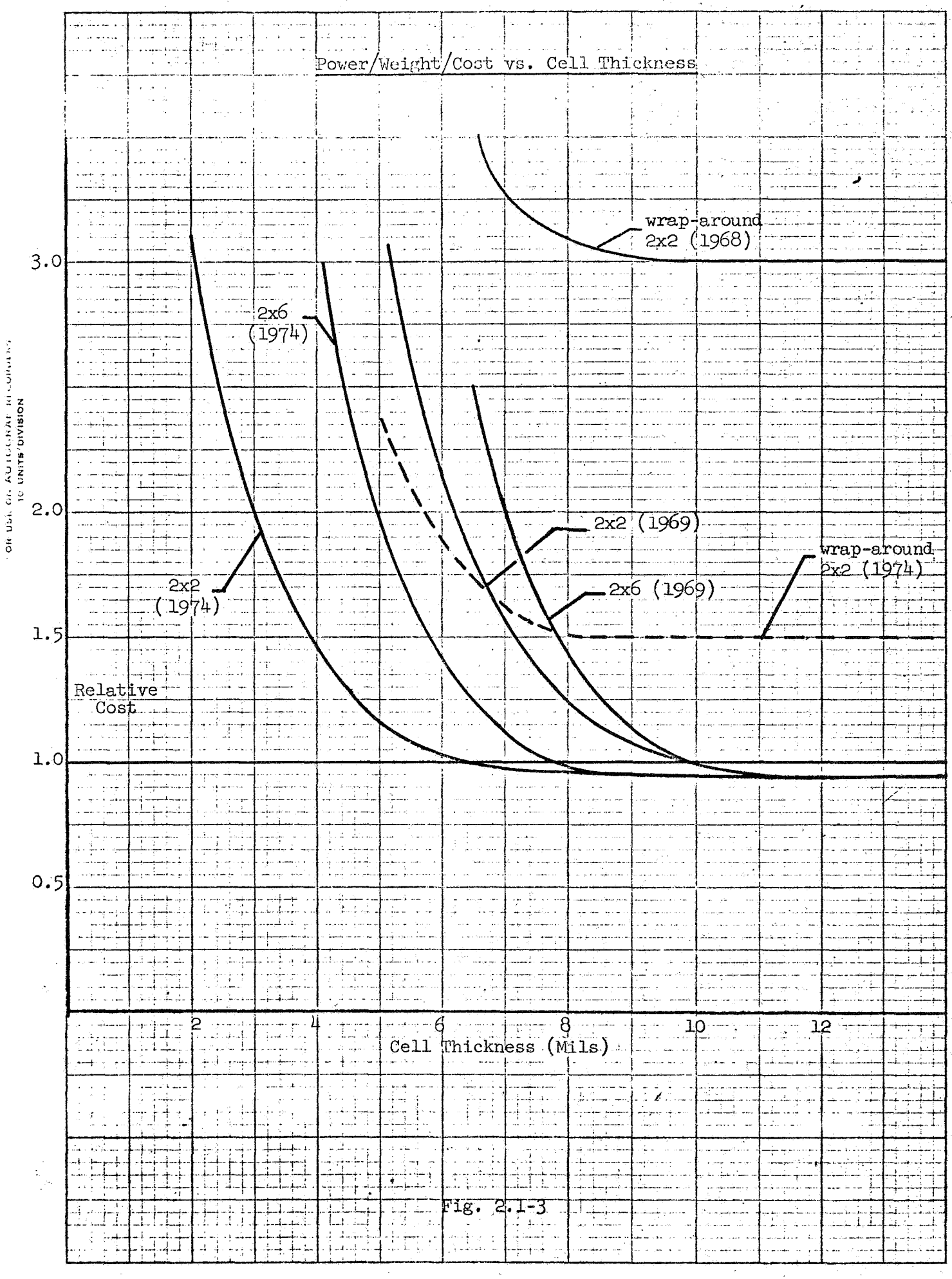
Power/Weight/Cost vs. Cell Thickness
wrap-around
2x2 (1968)
2x6
(1974)
2x2 (1969)
wrap-around
2x2 (1974)
2x6 (1969)
2x2
(1974)
Relative
Cost
3.0
2.0
1.5
1.0
0.5
2
4
6
8
10
12
Cell Thickness (Mils)

Fig. 2.1-3

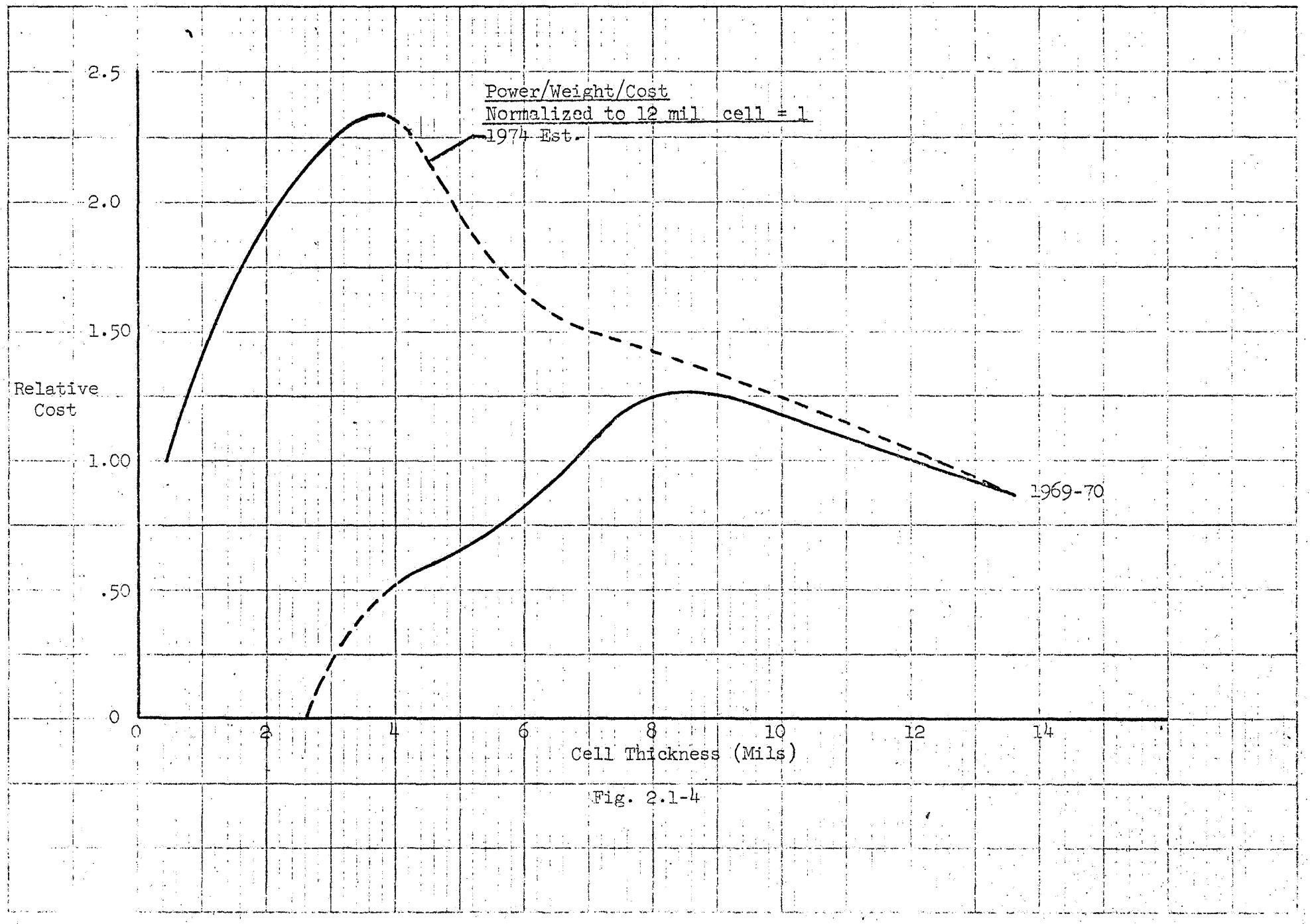

Fig. 2.1-4

weight/cost date for various types of cells as a function of cell thickness. A curve representing present-day conditions and one for estimated conditions in 1974 are shown. These are again normalized to the present-day 12 mil cell. The present-day curve indicates that the 8 mil cell appears optimum, with a shift to the 4 mil cell in approximately 4-5 years. Again, since the newer type cell prices reflect the requirement of a learning period, any increase or decrease in emphasis of effort in these area will greatly effect the period of time required before they reach the basic line conditions and become straightforward production items.

2.2 COVERSLIDE ASSEMBLY STUDY

2.2.1 Introduction

The purpose of this segment of the integrated array study was to develop an inexpensive lightweight solar cell cover. Present techniques of cementing and cleaning individual covers is a costly process with the least expensive version costing about $1.75 per 2 x 2 cm cell. This cost is based on a system that will fulfill the less strenuous near earth requirements. The advanced concept being considered utilized a continuous glass ribbon process and should reduce the cost by about 50%. The weight saving to be realized would be on the order of 60%.

The study was divided into two phases; the first was adhesive selection and the second was glass selection and a glass trimming technique.

Required adhesive properties are:

1) Good light transmission
2) Long Term environmental stability
3) Adaptability to automated assembly.

State-of-the-art adhesives that were considered were RTV 602, Sylgard 182, Dow Corning XR6-3489, G.E. SR 585 contact adhesive, and Schjeldahl GT 100 film adhesive, 1 mil thick. The fluid adhesives were applied by spraying both the cell and cover and by applying a metered quantity of adhesive to the cell. The cover was positioned on the cell and then was rolled with a pressure of 500 grams on a one inch wide, one inch diameter roller to achieve the desired thickness of one to two mils and to remove bubbles between the cell and cover. The Sylgard 182 and Dow Corning XR6-3489 proved to be most satisfactory in this study and the metered bead of adhesive method was more satisfactory than spraying.

The second phase of this task was concerned with glass selection and a glass trimming technique. This concept involves the use of a continuous ribbon of glass cemented to a continuous string of solar

cells and then trimmed to size after the cement has been cured. The concept of a continuous process of coverglass application used a Corning Glass type 8871 ribbon glass. This is a high lead content glass used for fabricating precision capacitors. It is available in a continuous ribbon form in various thicknesses ranging from 0.0013 to 0.0018 inches. The manufacturer stated that other types of glass including 0211 microsheet could be made in this form if sufficient quantities were required. Preliminary tests and sample assemblies indicated that this material configuration could enhance the cost and weight merit factors of large area lightweight solar arrays. The major problems with the concept was sizing the glass and the fact that ordinary handling techniques were inadequate. In order to avoid high breakage during handling of the glass it was decided to investigate the possibility of bonding the glass to the cell as a continuous process and trimming away the excess glass. Three methods of trimming the excess glass were evaluated in this study.

The first method consisted of a nichrome wire held taut between two insulated posts. Sufficient current was passed through the wire to maintain a temperature of 750°C. This wire was passed along the solar cell edge with a slight shearing motion to avoid excess glass building up on the cell edge. The art was accomplished easily but this method was discarded because there was a high cell rejection rate due to edge defects.

The second method consisted of using a high velocity jet of abrasive particles 25 microns in diameter at 80 pounds per square inch air pressure, using a gun with a nozzle diameter of 0.006 inches. This method produced the second highest reject rate, but is still being considered for a backup technique.

The third and most successful method uses a diamond scribe with a 1/2 to 1 mil radius point and a pressure of 30 grams. The procedure consists of drawing the scriber across the glass surface and lightly scoring the surface. The glass is then bent and broken along this line.

2.2.2 Adhesive Study Results

The purpose of this study was to select an adhesive capable of bonding 0.0013 inch thick ribbon glass to a silicon solar cell. The system was also required to be readily adaptable to an automated process. The investigation was carried out with the intent of comparing several new adhesive types with existing types with the various tests developed for this application.

Before any tests were actually conducted, an investigation of manufacture specifications was made. The criteria for selection were cure temperature ranges within - 100°C to + 100°C, rapid cure time, adhesion upon contact if possible, and transparency. Upon completing this phase the following candidate adhesives were selected:

1) Sylgard 182 (Conventional adhesive)
2) RTV 602 (Conventional adhesive)
3) XR6-3489 (Conventional adhesive)
4) Schjeldahl GT 100 (New application)
5) SR 585 (New application)
6) RTV 3140 (New application)

These adhesives represent a broad range for the application. Sylgard 182 requires a catalyst and cures very slowly at room temperature (about 1 day). However, it cures very rapidly when heat is applied (2 minutes at 200°F). RTV 602 has a pot life of approximately one hour at room temperature and cures very quickly when heat is applied (1 minute at 200°F). XR6-3489 is a purified version of Sylgard 182 and possesses much the same properties. Schjeldahl GT 100 is a sheet adhesive which melts and bonds when heat is applied (250°F). SR 585 is a contact adhesive which has an optional catalyst. It is to be completely cured before bonding. This takes about one day at 300°F. In the first approach used to study adhesive application methods, each adhesive was prepared, according to manufacturer's specifications, and applied to the cell with a syringe. Each cover slide was rolled onto the cell to insure a uniform bond free of bubbles and eliminating any excess adhesive between the cell and glass. Roller pressure was

approximately 500 grams for a one inch wide one inch diameter roller to avoid breaking the cell.

In the second approach, each adhesive with the exception of Schjeldahl GT 100 was thinned to a consistency suitable for spraying. The adhesive was sprayed on both the cell and the cover. The ratio of thinner (Naptha) to adhesive, by weight, was about 3:1 in each case.

As a third application the ribbon glass was coated on one side by passing the ribbon over the adhesive container so that only one side was wetted, the adhesive being thinned again 3:1 by weight. This was found to be a good consistency for coating to avoid either puddling or running after coating. This was the third possible application to production line assembly. As a final step for the last two applications the coated glass was exposed to 29 inches of vacuum at room temperature to eliminate any air bubbles present in the adhesive. If this was not done the possibility of outgassing would exist between cell and glass when bonded and subjected to thermal vacuum. The glass was then rolled on the cell as described previously.

After assembly, each specimen was exposed to heat and vacuum (300°F and 29 inches vacuum for 30 minutes). This was done to inspect for any outgassing between cell and glass severe enough to cause visible bubbling of adhesive. Bubbles would, of course, be undesirable as a possible nucleus for delamination and from additional outgassing.

2.2.2.1 Conclusions

Sylgard 182 and XR6-3489: These adhesives showed very good cure characteristics. They could be cured to a workable adhesive in about two minutes at 200°F. This appeared to be independent of the amount of thinner added. This was due to the fact that at this temperature the Naptha would boil off in a period of approximately 20 seconds. It appeared promising from a production line viewpoint.

Applying the adhesive revealed no problems. The adhesive would give a uniform even coating when dipped and the excess squeezed off. Pressure was applied at about 1 lb/inch to remove enough excess to avoid large amounts of waste when later rolled on at 10 lb/inch.

These two combinations resulted in an adhesive layer of about 1 mil. When the adhesive was sprayed (thicker than 1 mil) it could be squeezed and rolled onto the glass with the same results: no visible outgassing under 30X magnification after thermal vacuum exposure. In summary, these two adhesives were very good in every aspect.

RTV 602: This adhesive also showed very good cure characteristics. It would set up in about one minute at 200°F. Like the 182 and XR6-4589 the Naptha content didn't seem to effect this time.

The 602 could be handled in much the same manner as the 182, but required greater speed. This was due to its instability at room temperature. At room temperature in small quantities it begins to jell in about 10 minutes. Because of this it was almost impossible to spray any quantity of samples without the spray gun clogging. No amount of thinner would effect this. This same problem occurred when applied through the syringe or dipped. This is very undesirable for the automated assembly line case because a quick cure is desired only when heat is applied.

No visible outgassing was apparent under 30X magnification after thermal vacuum exposure.

RTV 602 appears very marginal in automated assembly application.

Schjeldahl GT 100: This adhesive, when placed between a solar cell and coverglass and heated to 250°F would melt and bond the cover to the cell. Large bubbles 30 to 40 mils in diameter and usually three or more would be formed by the entrapped air. About half these bubbles could be rolled out while the adhesive was still in a fluid state. Because of this bubble generation the sheet adhesive concept appears inferior.

General Electric SR 585 Contact Adhesive: This adhesive is readily adaptable to the ribbon glass tape concept. If the adhesive is applied to one side of the ribbon glass and cured properly the resulting pressure sensitive tape may be applied to a solar cell. Initial samples formed a great many bubbles when subjected to a thermal vacuum of 300°F and 29 inches. The bubble problem was

eliminated by subjecting the adhesive to a more thorough cure in a 29 inch vacuum at 300°F for one to eight hours. After this cure the glass tape was rolled on the solar cells to minimize air entrapment. Rolling pressure was about ten pounds on a one-inch wide roller. The adhesive thickness was approximately 0.001 inches. Adhesive was applied to the ribbon glass using a surface dip technique. Completed samples were subjected to a thermal vacuum of 300°F and 29 inches vacuum to determine if additional bubbles would be formed under the cover. After a two-hour exposure additional bubbles were observed so this system has been rejected.

2.2.3 Trimming Procedure Results

The objective of the trimming procedure investigation was to gather sufficient date to determine which of three glass trimming techniques would be most adequate. The three methods investigated were a hot wire, abrasive or sandblasting and the diamond scribe.

Samples consisted of five cells bonded to an adequate length of ribbon glass to simulate a continuous process model. Distance between the cells in this test was approximately one cell width. In actual practice this distance would be much less, about 0.100 inches. The glass was bonded using the Sylgard 182 adhesive bead technique previously mentioned. Bond line thickness varied from two to three mils. This bond line thickness must eventually be reduced to one to two mils if the weight objective is to be achieved.

The quality of the trimmed edges was based on typical edge chip and corner chip criteria. Acceptable edge chips were 0.015 inches in from the cell edge and 0.150 inches long. Acceptable corner chips were 0.020 inches on a leg. Chips exceeding these dimensions were considered unacceptable.

2.2.3.1 Hot Wire

A 0.030 x 0.005 inch nichrome ribbon was heated to approximately 750°C and passed along the edge of the covered cell, thus cutting off the excess coverglass. Cutting speed was 12-15 inches per minute.

Preliminary results appeared very promising until a comprehensive microscopic examination was performed. The hot wire vaporized some of the silicone rubber adhesive during the cutting operation which left a very heavy ash deposit on the glass. Removal of this ash caused excessive damage to the edge of the glass. The hot wire also became coated with an excessive quantity of glass after about six cuts along the 0.788 dimension of the cell. This accumulation hampered cutting and had to be continually removed before additional cutting continued. There was concern that the process may cause electrical degradation. Therefore, I-V curves were taken for the cell to determine if any degradation had occurred in the electrical characteristics due to effects of the hot wire on the cell edge. Two typical curves are presented in Figures 1 and 2. Although there was a detectable change it was not considered significant. Figure 2.2-3 is a photograph of a hot wire trimmed cell which shows another detrimental aspect of the hot wire technique; that is, the formation of bubbles under the glass surface. This bubble formation was due to a momentary pause in the cutting stroke thus indicating a critical process variable.

Figures 2.2-4 and 2.2-5 (photographs) illustrate examples of acceptable and unacceptable hot wire trimmed edges based on the specification previously defined.

2.2.3.2 Abrasive Cutting

This coverglass trimming technique uses a small high velocity jet of abrasive particles to trim the glass. This equipment is essentially a subminiature sandblaster using abrasive grit 25 microns in diameter propelled by an air pressure of 80 p.s.i. through a nozzle 0.006 inches in diameter. The nozzle was 0.015 inches above the glass surface. Cutting speeds of thirty inches per minute on the 1.3 mil glass were obtainable. The only difficulty occasionally encountered with this method was the degradation of the cell junction. This was due to erosion of the cell edge if the abrasive stream was not directed precisely. Some halo effect due to overspray of the abrasive was noted on the glass adjacent to the cut, but effects on cell output

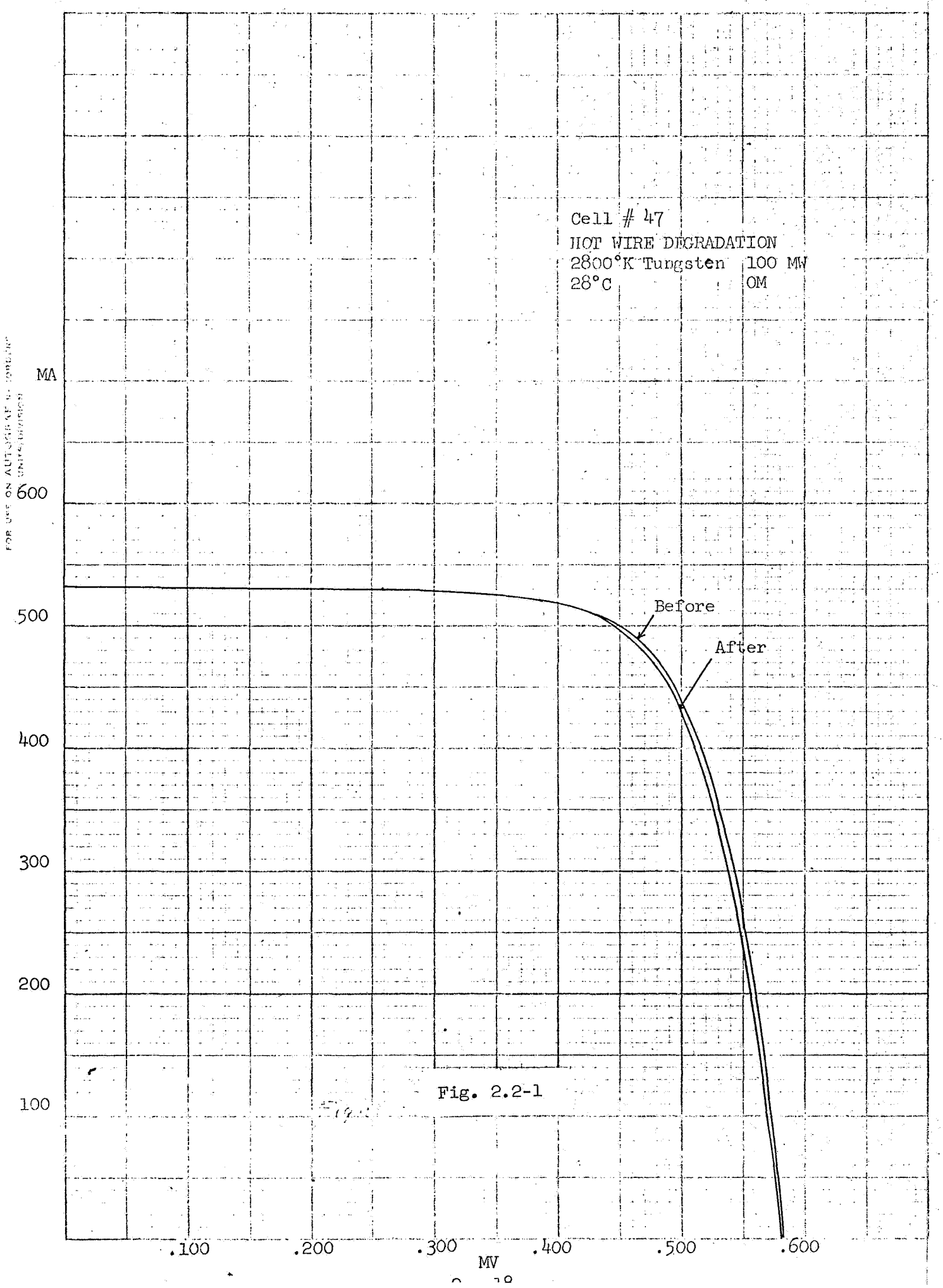
Cell # 47
HOT WIRE DEGRADATION
2800°K Tungsten 100 MW
28°C OM
MA
600
500
400
300
200
100
Before
After
.100
.200
.300
.400
.500
.600
MV

Fig. 2.2-1

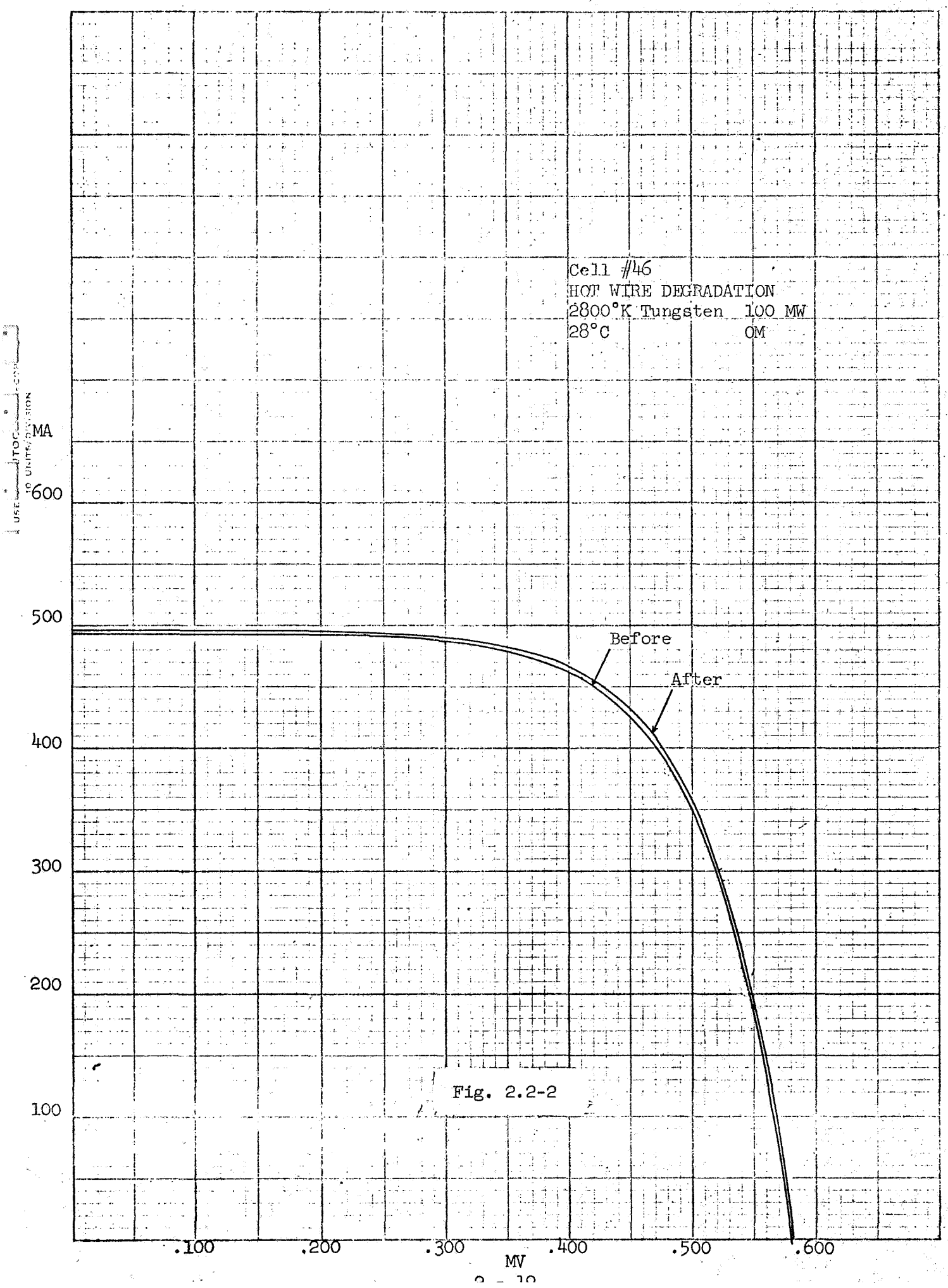
Cell #46
HOT WIRE DEGRADATION
2800°K Tungsten 100 MW
28°C OM
MA
600
500
400
300
200
100
Before
After
.100
.200
.300
.400
.500
.600
MV

Fig. 2.2-2

Fig. 2.2-3 Acceptable
(50x) Cell on right side

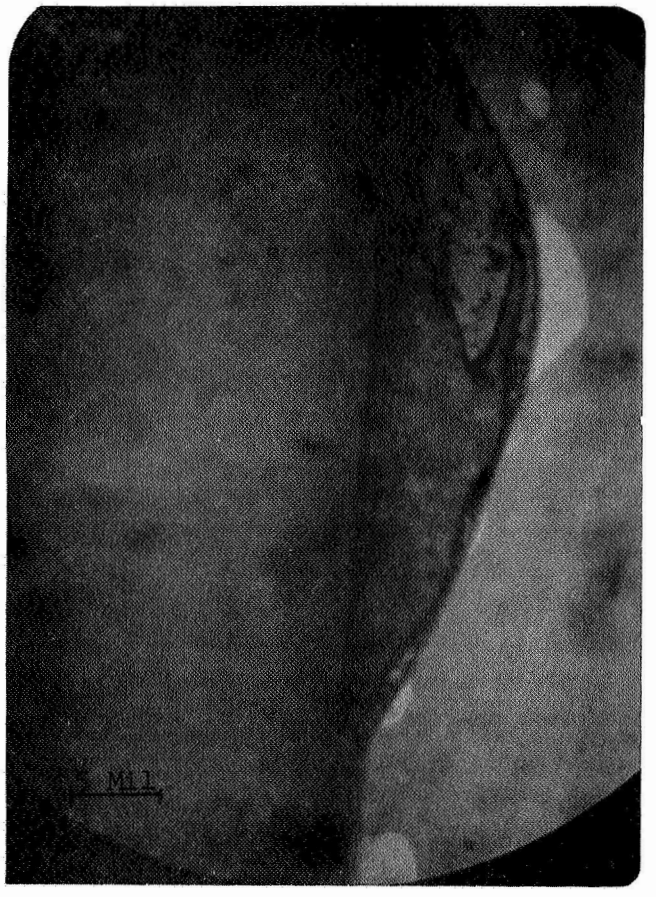

Fig. 2.2-4 Unacceptable
because of glass chip
(50x) Cell on right side

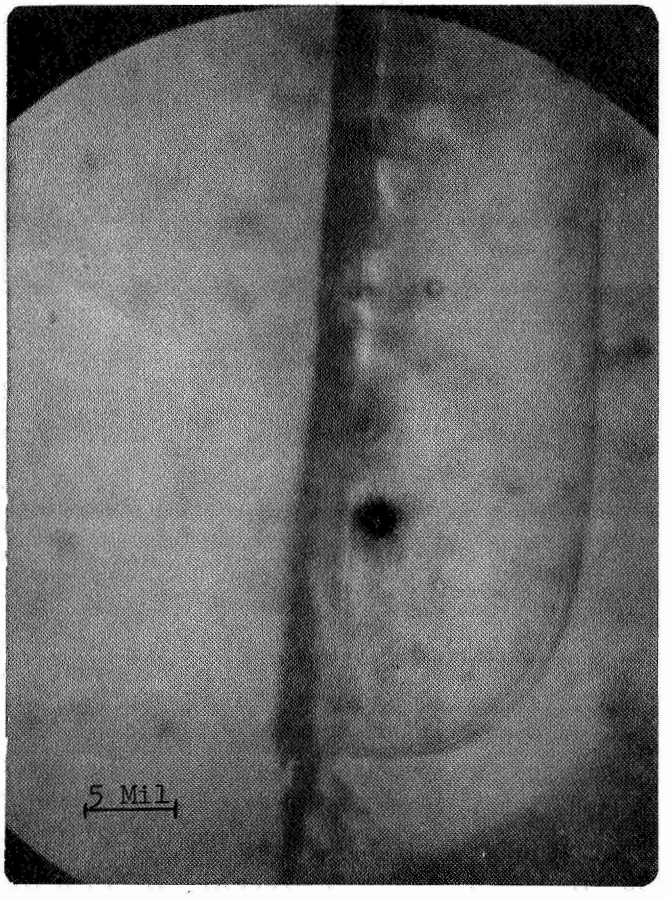

Fig. 2.2-5 Bubble caused by overheating
(50x) Cell on right side

were not detectable. It is felt that these alignment problems could be ultimately overcome and this system should be retained as a potential process technique. Figures 2.2-6 and 2.2-7 illustrate examples of acceptable and unacceptable cuts performed by the abrasive trimming technique.

2.2.3.3 Diamond Scribe

This method of sizing the ribbon glass appears to be the most successful of the three processes investigated. This process consists of lightly scoring the surface of the glass and then bending the glass along the scored line until the fracture occurs.

The diamond scriber selected for this task was polished to a point with a 0.0005-0.001 inch radius. Thirty grams of pressure was applied to the scribe. In this test, scribing was performed under a 10X stereomicroscope so that precise control of the distance from the edge of the cell could be maintained. For a production process an accurately indexed tool would be used. This edge distance is relatively critical and must be held to five mils or less from the cell edge to avoid a random fracture of the glass.

Figures 2.2-8 and 2.2-9 illustrate examples of acceptable and unacceptable edges done with the diamond scribe. Table 1 summarizes a comparison of the results obtained when a large quantity of cells were processed with the three trimming techniques.

2.2.3.4 Conclusions

The feasibility of an automated coverglass assembly process is excellent and additional work will be performed to refine the concept and improve the yield of acceptable units. The adhesive that has been selected for additional study will be Sylgard 182 or XR6-3489. Trimming studies will be continued using the diamond scribe trimming technique.

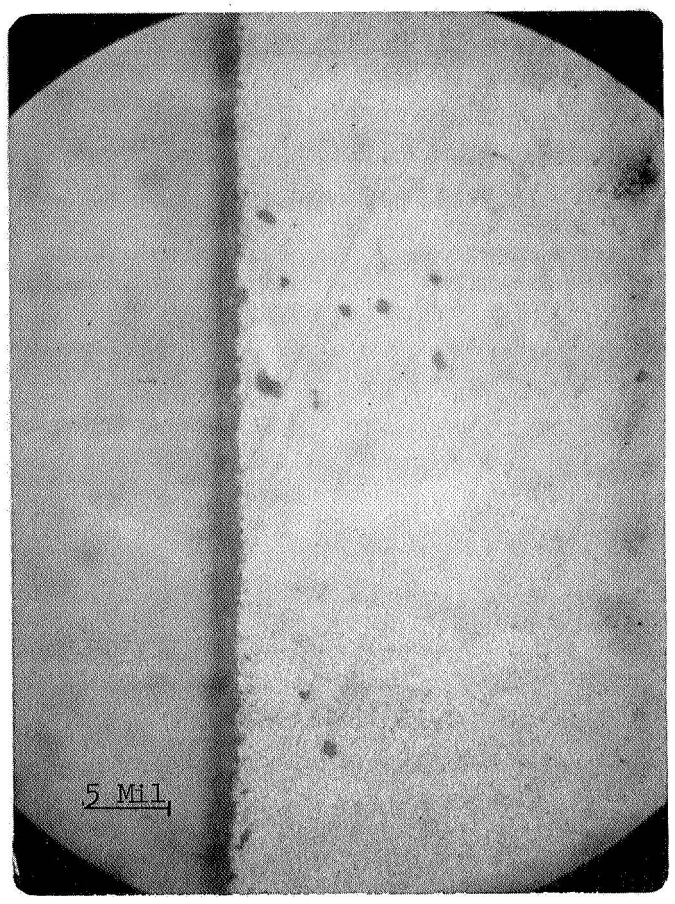

Fig. 2.2-6 Acceptable abrasive cut (50x) Cell on right side

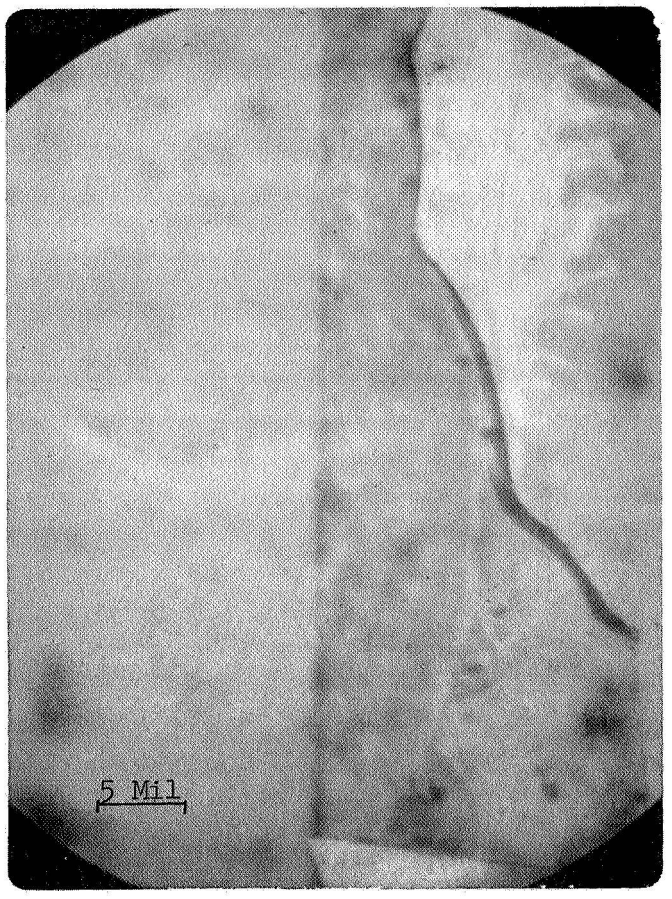

Fig. 2.2-7 Unacceptable abrasive cut (50x) Cell on right side

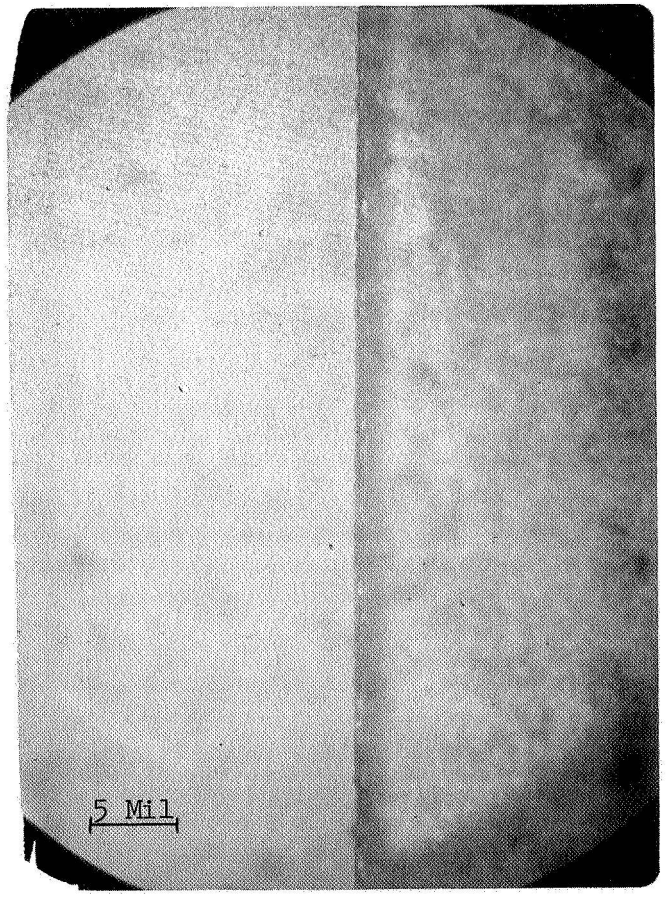

Fig. 2.2-8 Acceptable scribed break (50x) Cell on right side

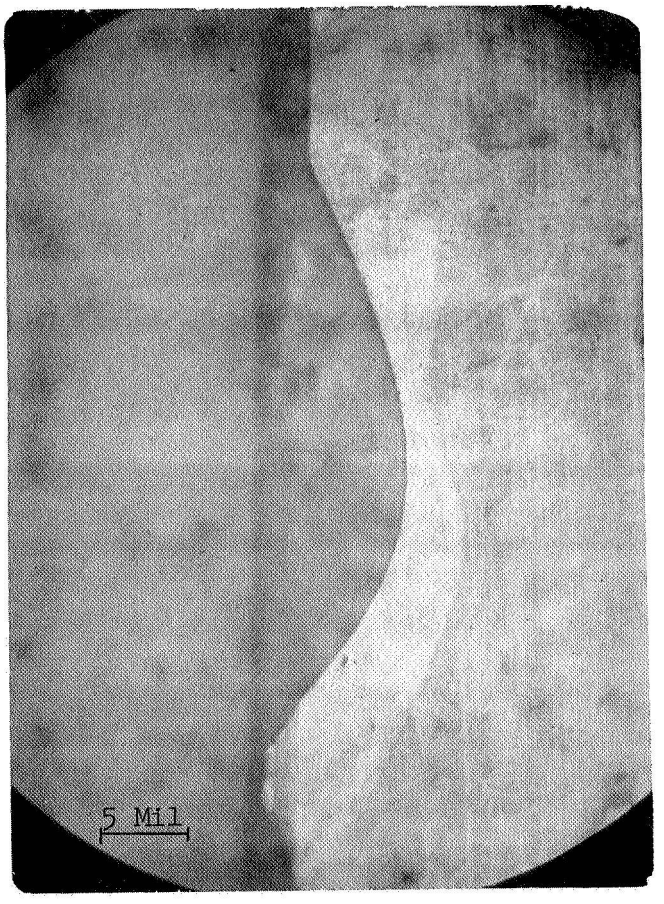

Fig. 2.2-9 Unacceptable scribed break (50x) Cell on right side

Mechanical Inspection of Trimming Tests

Trim Technique	No. of Samples	Side Trim			End Trim		
		Good	Bad	% Good	Good	Bad	% Good
Hot Wire	44 cells 88 sides	14	74	16	8	36	18
Abrasive	35 cells 70 sides	31	39	44	21	14	60
Scribing	86 cells 172 sides	87	85	51	52	34	61

Table 1

2.3 SOLAR CELL INTERCONNECT STUDY

2.3.1 Interconnector Study

During this report period a stress analysis of solar cell interconnectors was conducted. This analysis investigated not only the manner in which stresses could be expected to distribute themselves throughout the array, but also defined environmental parameters which can be utilized in interconnector design. It was assumed that the principle utilization of the interconnector would be in terms of electrical continuity, and that actual structural strength should be provided for by the array substrate. The analysis consists of six parts.

1) Stress distribution in the array
2) Thermal expansion motion
3) Thermal cycling fatigue
4) Vibration fatigue
5) General model for stress loops
6) Alternate loop concepts.

2.3.1-1 Stress Distribution

For present day state-of-the-art conventional array the substrate can be characterized as rigid. In more advanced designs, as the overall substrate weight was reduced the substrate rigidity was also diminished. In the present study the substrate of concern is a 1 mil polyimide Kapton H film substrate and rigidity is almost nonexistent. As a result, the stress distribution across the array will be expected to be quite different from the present day rigid substrate. Environmental loads, thermal and vibrational, will be transmitted through the substrate, interconnector, cell adhesive, and cell. The coverglass assembly can most likely be ignored although in some designs one could conceivably couple stresses in the coverglass assembly to the entire panel through the solar cell. In this examination however, the coverglass assembly will be neglected.

In order to qualitatively understand the panel behavior under stressing the spring rates K, can be calculated for the simple case of solar cell,

interconnector, and substrate. It will be assumed for the present that the cell adhesive can be neglected as a stress relieving means. For any large panel, i.e., one meter^2 or greater, the approximation should be viable. A schematic for a representative system is shown below. This approximates the interconnector as a straight segment parallel to the substrate. For the spring rate calculations this is quite accurate.

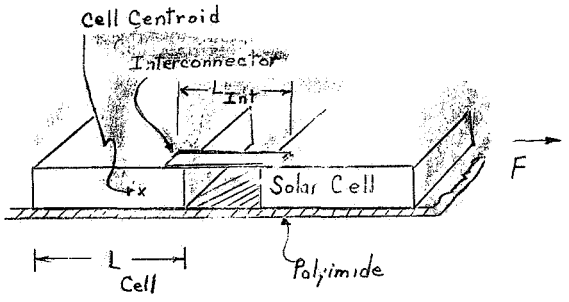

A gap of 0.017" between cells will be assumed. The cells will be nominally 0.788 x 0.788" silicon cells. A total interconnector width of 0.100" at a thickness of 0.002" will be examined. For this analysis the cells will have a polyimide substrate completely covering the back. The polyimide substrate will have an area defined as 0.394 + 0.017 + 0.394 = 0.805" length and 0.788" wide with a thickness of 0.001".

The spring rate K is given as $F \div s$ or $\frac{btE}{L}$ Eq. 2.3-1

Where $s = \frac{FL}{btE}$ = stress and F is the applied force, t and b are the material thickness and width respectively.

E is the modulus of elasticity for the material element, and L is the length.

$$K_{\substack{\text{substrate} \\ \text{polyimide}}} = \frac{(.788)}{.805} (.001) (4.3 \times 10^5) = 4.2 \times 10^2$$

$K_{\text{substrate}}$ $= \frac{(.788)}{.805}(.01)(10.5 \times 10^6) = 1.0 \times 10^5$

.010" aluminum
instead of polyimide

$K_{\text{interconnector}} = \frac{(.100)(.002)(10.5 \times 10^6)}{.017} = 1.0 \times 10^4$

.002" aluminum

Any force f, applied to the substrate or interconnector will produce a deflection X, satisfying $f = KX$. Correspondingly, the application of a deflection X to the material will require the use of a force f, given by the above relationship. What this means is that a force f will produce a strain S in the substrate such that $S = \frac{f}{K_s}$. If the interconnector must then also absorb such a strain then it must experience a force $f_i = K_i S$. For the case of an aluminum substrate and an aluminum interconnector as described above $f_i = K_i \frac{f}{K_s} = \frac{1}{10} f$. Thus, whereas the rigid substrate (i.e., aluminum substrate) provides a system in which the substrate absorbs the major part of stresses (i.e. $K_i/K_s = \frac{1}{10}$) the spring rate for the polyimide substrate (i.e., $\frac{K_i}{K_s} \simeq 20$) indicates that unless stress relieving is utilized, the applied forces will be absorbed almost totally by the interconnector.

However, if stress relieving is utilized so that the interconnector can be ignored as a stress member, then all stresses can be distributed through the substrate which is what is needed for a reliable interconnector design. Also, comparing spring rates for rigid aluminum substrates (10^5) and polyimide substrates (4.2×10^2), they indicate that much greater expansion will be experienced for a given force by the polyimide substrate.

To further describe the above system a simple approximation to the array system can be imagined as a system of springs $K_i >> K_s$.

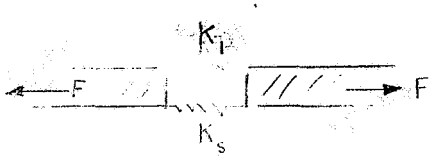

It is obvious that forces applied to the system will cause the system to behave essentially as if only K_i existed, unless stress relieving is employed such that K_i effectively becomes zero.

Furthermore, unless the array is somehow constrained to be in a flat plane, the applied forces, either through vibration of thermal effects, will tend to cause bending of the array out of a flat plane because of the unequal torques due to the system of K_i and K_s. Therefore the problem of designing an interconnector system reduces to one of eliminating the interconnector as a stress member. This typically is done by providing a stress loop which allows cell movement with restraint provided only by the substrate. The amount of cell movement that must be accounted for varies depending on the cause of movement.

The extent to which the interconnector, cell, and substrate could be expected to expand (contract) under temperature cycling can be reasonably calculated for the polyimide substrate case. To this end, a worst case approach will be employed to examine stresses in the interconnector due to thermal conditions. At the present time a thorough investigation of the vibrational loads cannot be conducted because of the lack of stowed configuration characteristics, however work on roll up arrays have provided some anticipated substrate stresses that will be utilized to determine approximate cell motion values. The problem of interconnector design will therefore be based on cell motion in general, with specific emphasis placed on motion associated with thermal effects. Then once a design model is obtained, a general description will be made of how vibrational effects can be accounted for.

2.3.1-2 Thermal Expansion Motion

It will be assumed first that no interconnector is attached to the cell and only the substrate expansion will be examined. This expansion value can then be used to design a suitable stress relieved interconnector. The expansion of the array can be considered from two views. First, if the substrate is bonded rigidly to all parts of the cell it

will expand as a unit with the cell. In this model the intercell spacing is changed only by the substrate expansion associated with the small spacing between cells. At the other extreme, it can be assumed that the cells "float" with little rigidity between substrate and cell. Then the substrate expansion occurs with respect to the centroid of adjacent cells. This model will produce a much greater intercell spacing change. These two extreme cases produce different cell motion values which are calculated below.

Case I Substrate rigidly bonded to the cell.

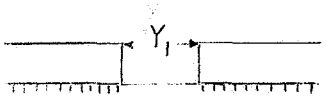

The change in substrate length is then $\Delta Y_1 = Y_1 \alpha_k \Delta T$ Eq. 2.3-2

α_k = coefficient of thermal expansion for Kapton H film

ΔT = temperature change in °C

Y_i = 0.017 inch for a typical array

It is assumed that panel fabrication will occur at about 28°C. Hence, the ΔT will be 100-28 = 72°C, using 100°C as a typical high temperature value.

Therefore $\Delta Y = (0.017") (2 \times 10^{-5}$ in/in°C) (72°C)

$= 2.5 \times 10^{-5}$ in.

Case 2 Substrate expands with respect to centroids of adjacent cells.

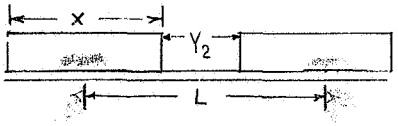

Here, $\Delta L = L \alpha_k \Delta T$ $\quad L = 0.394 + 0.394 + 0.017 = 0.805$

$\Delta X = X \alpha_{si} \Delta T$ $\quad X = 0.788$

$\Delta Y_2 = \Delta L - \Delta X$ $\quad \alpha_k = 2 \times 10^{-5}$

$\alpha_{si} = 7.2 \times 10^{-6}$

Therefore

$\Delta L = (0.805) (2 \times 10^{-5}) (72) = 11.6 \times 10^{-4}$ in.

$\Delta X = (0.788) (7.2 \times 10^{-6}) (72) = 4.1 \times 10^{-4}$ in.

and $\Delta Y = 7.5 \times 10^{-4}$ in.

Hence, depending on the characteristics of the adhesive between cell and substrate, an expansion between 2.5×10^{-5} in. and 7.5×10^{-4} in. can be expected to occur upon heating to 100°C. A similar calculation for cooling to a typical value of - 100°C yields a contraction distance varying from 4.4×10^{-5} in. to 13.3×10^{-4} in. With these values a minimum requirement for a stress loop is obtained by requiring that much more interconnector length. Empirically, thermal cycle tests have shown that this minimum interconnector loop is not satisfactory. This discrepancy is due to fatigue effects incurred through repeated flexing of the interconnector and this problem will be discussed later using the above values for cell motion as minimum design goals. A more

precise calculation of stress relief length would include a complete examination of vibrational effects and twisting of the interconnector due to motions perpendicular to the Y direction, with further corrections for the fatiguing properties of the interconnector material.

If we go back to the situation where no stress relieving is employed in the interconnector, thermal changes will not stress the interconnector to any large degree due to the relatively low spring rate of the substrate. In other words the substrate would buckle or stretch to comply with the interconnect length change thus transferring all of the external array forces from the substrate to the interconnector. Vibrational bending and twisting loads could then impose severe stresses in interconnector and interconnector bond regions.

For the case of a direct diagonal interconnect,

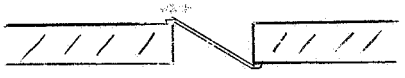

the stresses could lead to high fatigue rates at the cell edges. Similarly with a common stress relief loop

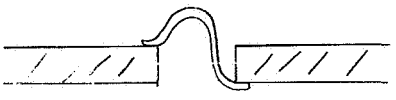

consideration must be taken of the fatigue due to bending as a result of cell movement.

By using a wrap-around interconnector or a wrap-around cell contact these bending fatigue failures can be essentially eliminated. In this case all loads are carried in a basic stress-strain mode with the interconnector and substrate being intimately bonded so they act as a single stress member and metal interconnector thickness can be made extremely thin to minimize stresses in the metal across the cell gap.

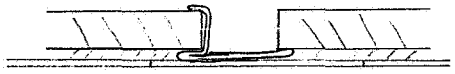

Fig. 2.3

For this wrap-around configuration, the design must consider primarily plane stress/strain characteristics in the interconnector and substrate and shear loads on the bond region. For the situation of simple thermal motion then, the wrap-around interconnector avoids the bend fatigue associated with diagonal interconnects or stress relieving loops. Various approaches to a system of interconnectors do exist. The actual configuration depends on the total array configuration and environment. Although short term direct stresses are not as important in a system with stress relieving loops, experience has shown that repeated bending and flexing as would be expected in a flexible array can impose fatigue failures.

2.3.1-3 Fatigue Failure - Thermal Cycling

As calculations in the previous section indicated, the actual amount of excess length required for stress relieving an interconnector is relatively small and typically is on the order of a few mils. However, in many cases where more than this minimum extra length is utilized, failures in the interconnector under thermal cycling do occur. The explanation of this apparent discrepancy is that fatigue occurs in a material where relatively low level stresses are experienced in cycling. The present investigations will therefore look at the type of stress levels which can produce fatigue failures, correlate these stresses with actual cell motions, and examine various concepts for minimizing the possibility of fatigue failures.

Again, array loads are to be expected, basically from two sources. These consist of short term and relatively severe vibrational loading and long term, relatively mild, thermal loading. Of these two the vibrational problem is the most complex. Not only does it depend upon the environment and structural materials, but also the structural and stowage configuration. As a first approximation then, the analysis will be based on the thermal motions calculated in the previous section.

Earlier, the amount of cell motion in a thermal cycle of - 100°C to + 100°C was ascertained. From this value it is possible to determine the minimum excess amount of interconnector length required as a stress loop for protection against fatigue failure. (If vibrational motion were defined in terms of a similar cell motion then it also could be used as a design requirement.)

The basic model to be examined will consist of an array of silicon solar cells with an intercell gap of 0.017". This corresponds to the series gap presently used in other calculations in this study. The substrate will be 0.001" polyimide film. A further assumption will consider that the stress loop bend radius is 0.010". This also is a commonly used value in conventional designs and is compatible with the cell spacing value. The effects of altering this bend radius will be mentioned later, however as a general rule the following analysis of bending stresses will apply.

For a given piece of material the stresses incurred through bending are given by:

$$S = \frac{E \cdot X}{R} \qquad \text{Eq. 2.3-3}$$

where E is the modulus of elasticity, X is the distance from the center of bending to the stress point in question, and R is the radius of curvature. For a thin uniform interconnector the center of bending will lie in a plane located midway through the thickness of the interconnector. Obviously the maximum stress will be at the interconnector surface.

$$S_{max} = \frac{Ed}{R} \text{ where } d = \text{half thickness of the interconnector.}$$

Eq. 2.3-4

It is assumed that when the interconnector was bent to its assembly shape, it was subsequently annealed or the working left the part with essentially no residual stress buildup. Stresses will occur only with further bending. The actual amount of stress in the interconnector can be calculated in the following manner.

First the initial and final radii of curvature as a result of the cell movement are determined. The actual stress levels incurred through bending from the flat configuration to each of the desired radii are calculated. Then, the difference in these values yields the stress levels to which the interconnector will actually be subjected. Since fatigue is dependent upon a material's highest stress level the maximum stress as defined earlier, will be used. Therefore,

$$S_f = \text{fatigue stress} = Ed\left(\frac{1}{R_i} - \frac{1}{R_f}\right) \qquad \text{Eq. 2.3-5}$$

where R_i = initial radius (here equal to 0.010")

R_f = final radius

Earlier calculations indicated that the total cell movement from - 100°C to + 100°C would be $\pm$ 0.001 inches. For simplification it will be assumed that this total motion consists of a smooth

$\pm$ 0.001 inch motion about the pre-bent position.

Stress fatigue data is given as a curve, as a function of cycles to failure on a log scale for a particular material. The fatigue rate is dependent upon the actual stress levels experienced. For a typical material such a curve will have the characteristic like the sketch below. [2)]

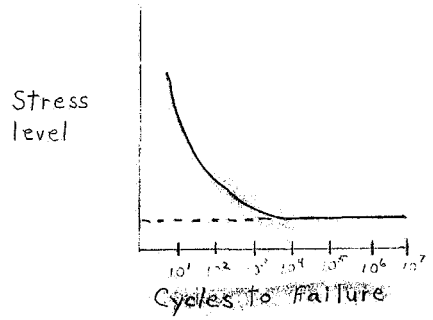

It is obvious that a slight increase in stress levels can often produce a dramatic decrease in the material lifetime. The endurance limit is therefore defined as that stress level for which essentially no fatigue will occur. As a practical matter, 500,000,000 cycles is usually used as the definition of no fatigue. In the above figure then, the endurance limit is shown as a dashed line. Under some circumstances, it may be possible to use significantly higher stress levels (50% or greater) with acceptable cycling lifetime, however, as a general rule one can realize only a small increase in stress levels (25%) before cycle lifetime becomes too short.

As an example, an interconnector thickness of 0.002" will be assumed (d = 0.001"). The interconnector material will be Aℓ 1100-0. The stress value for the material "endurance limit" will be used. As stated above this value indicates the cycle stress which a material can withstand without any failure occurring and characteristically represents no failures up to 500,000,000 cycles. Obviously for an

---

2) Metals Handbook, Vol. 1, eighth edition, American Society for Metals.

actual array this figure is not a reasonable design goal since a mission with 90 minute orbital period will have approximately only 6,570 cycles during each year's lifetime. But since the actual relationship of the fatigue stress for this number of cycles is not known a "built-in" safety factor will result in using the endurance limit. In the first configuration to be examined the stress loop will be placed with its center of curvature in the plane defined by the cell surfaces (i.e., there is essentially no expansion loop). In this manner, cell motion will be directly related to the radius change.

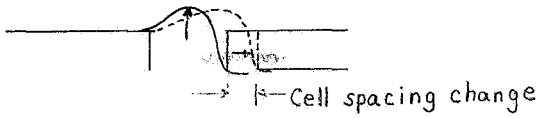

Since the initial bend radius is known, the maximum allowed change in radius without exceeding the endurance limit can be calculated as,

$$R_f = \frac{R_i}{1 - \frac{S_f R_i}{Ed}} \qquad \text{Eq. 2.3-6}$$

For a given system (Aℓ 1100-0 interconnector, with R_i = 0.010", $E = 10^7$ psi, thickness = 0.002" and S_f = 5000 psi)

$$F_{f_{max}} = \frac{0.010}{1 - \frac{(5{,}000)\ (0.010)}{10^7\ \ (0.001)}}$$

Hence, the maximum allowable change in curvature radius is 0.00005". This is obviously significantly less than the radius change to be expected from the 0.001" cell spacing change, which will produce a radius change on the order of 0.0005".

If we change materials and try 5050-0 aluminum which has a higher endurance limit with basically the same electrical properties and

fabrication properties we get the following results.

S_f can be increased to 12,000 psi, compared to 5,000 psi for Aℓ 1100-0.

$$R_2 = \frac{0.010}{1 - \frac{1.2 \times 10^4 (0.010)}{10^7 (0.001)}}$$

$$= 0.01012"$$

for a maximum radius increase of 0.00012".

This again is well below the actual expected change of 0.0005".

Since the stress levels decrease with increasing bend radii (E, d, and S_f remaining the same) the effect of a 0.020" bend radius will next be examined.

Again Aℓ 5050-0 will be used.

$$R_2 = \frac{0.020}{1 - \frac{(1.2 \times 10^4) (0.020)}{10^7 (0.001)}}$$

$$= 0.02048"$$

for a maximum allowed increase of 0.00048".

This value is compatible with the cell spacing change, but realistically must be considered a marginal design.

If a 2 mil copper interconnector is examined $E = 1.8 \times 10^7$, and $S_f = 11{,}000$ psi.

$$R_{max} = \frac{0.010}{1 - \frac{(11{,}000) (0.010)}{(1.8 \times 10^7) (0.001)}}$$

$$= 0.01006"$$

or an increase of 0.00006"

This value is only slightly better than for the case of Aℓ 1100-0 and a 0.010" bend radius. Hence, the copper interconnector offers no fatigue advantage over aluminum.

In summary, if the stress loops are placed such that the center of curvature lies essentially on the plane of the cell surfaces, it is evident that from a fatigue standpoint the minimum allowable change

in radii will be exceeded. This is evident from the diagram.

The approximate length of the stress loop is π R or 0.031" for R = 0.010". Hence, over the 0.017" gap there is an excess of approximately 0.014" of aluminum, which will easily allow for the $\pm$ 0.001" cell movements under thermal cycling. However, if the cells move by approximately 0.001" this would imply as a worst case that the radius of curvature for the loop increased by approximately 0.005", a value greater than any of the allowable stress levels calculated for on the basis of the endurance limit.

One way in which improved fatigue resistance can be obtained is to place the stress loop higher above the cell surface. In this manner there will be less change in curvature radius with linear cell motion in proportion to the loop height.

In order to examine the impact of the interconnector height reference will be made to the following sketch. This schematically represents an extended loop interconnector between cells A and B.

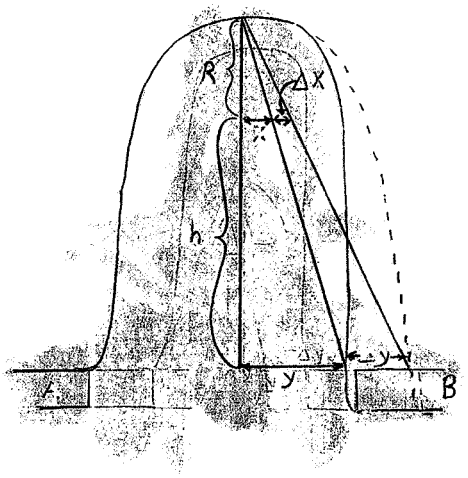

In this figure, Y is one-half the initial cell spacing distance and Δ Y is one-half the cell spacing change (assumed to be expansion for this derivation). h is the height from the plane of the cell's surfaces to the center of loop curvature. R will be the bend radius. Δ X will be identified as the change in bend radius.

Earlier it was shown that the change in bend radius must be limited to a maximum in order to prevent interconnector fatigue. The calculated values for the maximum change can now be used to obtain values of h with which the actual Δ Y values will form a compatible system, i.e., h must be determined such that for a given cell spacing change Δ Y, the bend radius change Δ R, (now identified with Δ X,) will fall within the endurance limits. This can be done in the following manner:

an identity $(X + \Delta X) - X = \Delta X$

define $h' \equiv h + R$ = total loop height

By similar triangles $\dfrac{X + \Delta X}{R} = \dfrac{Y + \Delta Y}{h'}$

and $\dfrac{X}{R} = \dfrac{Y}{h'}$

consequently $h' = R \dfrac{\Delta Y}{\Delta X}$ Eq. 2.3-7

Since Δ Y, R, and Δ X, are known from the design, h' (and obviously h) can be explicitly determined. Now we can solve for the design heights using the stress loops examples calculated before.

R = 0.010 interconnector is 2 mils thick copper.

$\Delta X_{max} = 0.00006$

$\Delta Y = 0.0005$

and,

$$h' = \frac{(0.010)\ (0.0005)}{0.00006} = 0.084$$

hence the no fatigue stress loop must have a total height of 84 mils in this case. This design is obviously poor because of the problems of working with such a high interconnect.

As a second example we might try the 2 mil thick 5050-0 aluminum alloy.

Again, $R = 0.010$ and $\Delta Y = 0.005$. Now however, $\Delta X = 0.00012$

$$h' = \frac{(0.010)\ (0.0005)}{0.00012} = 0.042$$

This implies a stress relief with a total height of 42 mils, a value which although better than the previous one, is still probably too high for a practical design.

At this point, knowing the pertinent quantities and relationships, we can attempt to optimize the interconnector system. Ways in which we can optimize the design for fatigue resistance include the following:

a) Utilize the thinnest interconnector practical.

b) Use alloys with the highest endurance limits within workable conditions.

For example, 5050-0 Aℓ alloy could be used in a one mil thickness instead of two mils; however, thinner interconnects that are self supporting are not likely to be practical.

Hence:
$$R_f = \frac{0.010}{1 - \frac{(12{,}000)\ (0.010)}{(10^7)\ (0.0005)}}$$

$$= 0.01024 \text{ inches}$$

for an allowable radius increase of 0.00024 inches.

This gives a value for h' given by

$$h' = \frac{(0.010)\ (0.0005)}{0.00024} = 0.021"$$

This value of 21 mils is still not a very desirable design requirement. These calculations therefore indicate that for preventing interconnector fatigue through cyclic thermal effects as specified, it is marginally possible to fabricate a suitable stress relieved interconnector. Obviously further fatigue resistance can be obtained with thinner interconnects, but we are thus faced with the need for either a laminated or deposited thin film interconnector on some high fatigue resistance substrate. In this respect, Aℓ on polyimide might be a good

candidate since the similar thermal expansion coefficient should minimize bi-material thermal stresses.

2.3.1-4 Vibration Fatigue

It should be recalled that the above calculations have been conducted with reference to thermal effects only; that increasing the temperature extremes will increase cell movement and subsequently interconnector stress levels. Based on vibrational tests by Ryan on a rollup array, vibrational motion on a lightweight polyimide film type array was found to incur cell spacing changes on the order of 4 mils. For such a case interconnector heights of 70-80 mils would be required to eliminate fatigue failures. This is obviously unacceptable. Although array vibrational motion is dependent upon the entire array configuration and method of storage, and this motion can possibly be minimized, it is reasonable to believe that such arrays will still experience cell motions in the 2-4 mil range. This will imply that conventional stress loops on the order of up to 80 mils will be required. This situation is not desirable and consequently alternate interconnector concepts are being considered. Before we consider other concepts however, one realizes that conditions do exist where a stress relieved interconnector will only have to account for small cell motions (approximately 1 mil) as with a rigid substrate design. For these cases it appears that it would be useful to provide a generalized relation for determining loop height based on interconnector material and thickness variables.

2.3.1-5 General Model for Stress Loops

Ultimately the problem of interconnector fatigue can be examined analytically to at least determine approximate design requirements. As shown earlier, the basic quantity in defining a loop requirement, is the cell spacing change ΔY. Our previous relation showed the loop height h', as

$$h' = R \frac{\Delta Y}{\Delta X} \qquad \text{Eq. 2.3-8}$$

Where R is the bend radius (assumed to be $\leq 0.010"$) and ΔX is the maximum allowed change in loop curvature radius, or

$$\Delta X = \left| R \pm \frac{R}{1 - \frac{S_f R}{Ed}} \right| \simeq R \left| \left(1 \pm \frac{}{1-\eta}\right) \right| \qquad \text{Eq. 2.3-9}$$

where $\eta = \frac{S_f R}{Ed}$ and the $\left| \quad \right|$ are meant to indicate that the absolute value will be understood.

This yields

$$\begin{aligned} h' &= \Delta Y \left| \left(1 - \frac{1}{1-n}\right)^{-1} \right| \\ &= \Delta Y \left| \left(1 - n^{-1}\right) \right| \\ &= \Delta Y \left| \left(1 - \frac{Ed}{S_f R}\right) \right| \end{aligned} \qquad \text{Eq. 2.3-10}$$

Hence, we have the generalized equation, so that given a cell spacing change of ΔY, and E, d, S_f, and R for the interconnector, an approximate value for the required "no fatigue" loop height can be calculated. Correspondingly, given a maximum value for h', and values for R and ΔY, a value for $\frac{Ed}{S_f}$ can be obtained. This can then be used to choose the proper material and thickness. In this manner a configuration can be examined during the design phase to determine whether or not a stress loop interconnector is practical.

2.3.1-6 Alternate Loop Concepts

The above calculations were based on the use of 0.010" or less bend radii. For larger bend radii the bulk of the interconnector is above and extends over the solar cell surface. This becomes impractical and the bend radius at the cell's top surface becomes very abrupt and would present a fatigue problem. (See sketch below.)

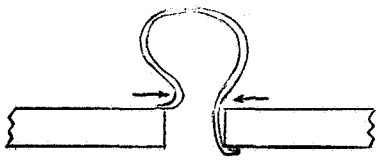

The magnitude of this shape problem is obviously dependent upon the initial cell spacing which has been assumed to be approximately 0.017".

Another alternative would be if the larger bend radius is accommodated by not placing the center of the loop above the cell surface, but rather below the cell surface. In the figure below a bend radius of 30 mils is assumed, such that the excess interconnector material is sufficient for approximately 1 mil cell motion. This configuration will be referred to as a "direct loop."

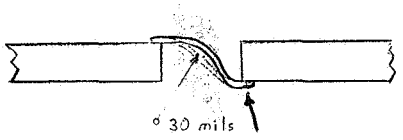

In this case, however, actual interconnector flexing is no longer centered at the top of the loop, but rather bending will occur all along the interconnector and in particular, at the cell bottom. If more material is utilized (corresponding to a smaller radius) to allow for motion of approximately 2-4 mils as could be expected under vibration, stress will be concentrated primarily near the cell bottom.

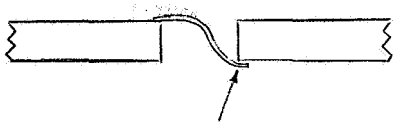

With the "heightened" loop we would also have a small bend radius, however cell motion induced stresses would be concentrated primarily at the top of the loop. With the "direct loop" described above, interconnector motion will now be much more evident near the cell's bottom surface and the fatigue situation will be effectively transferred from the top of the pre-bent loop to the bend next to the cell bottom.

This transfer of fatigue location will similarly occur in the situation of a heightened stress loop with a bend radius greater than 10 mils. Hence, the desire to use larger bend radii as an alternative to high stress loops actually only relocates the center of flexure fatigue to different portions of the interconnector. Again, this is dependent upon the initial cell spacing which has been set at 0.017" for this analysis. In the case of relatively small cell movements, or low cycling numbers (which is typical of most array designs used today), the calculations indicate that with optimum materials, fabrication, and assembly, this type stress loop can be constructed with good reliability. However, with the more gross motions expected with a polyimide substrate, and the practical matter of small interconnector flaws due to etching, bending, and general handling, confidence in a no fatigue interconnector system can be attained only with impractically high stress loops.

Summary and Conclusion

The concept of interconnector stress relieving does not appear to offer a good solution due to the anticipation of the occurrence of interconnector flexure fatigue failure for a flexible substrate. That is, within the array system concept presently conceived, a stress relieved interconnector, from the point of view of flexure fatigue, can only be considered a marginal system. The major problem is one of high stresses arising through cyclic bending of the stress relieving interconnector--a necessary consequence of the stress relieving concept. Yet, avoidance of these high stresses necessitates unwieldy configurations. Because of this inherent trade off, a more promising approach may be the

wrap-around interconnector mentioned earlier. The wrap-around solar cell contact (not to be confused with the wrap-around interconnector) offers the ultimate solution here from a conceptual point of view. From a practical point of view however, the wrap-around interconnector appears to be a more immediate and practical solution. With the wrap-around type mechanisms stress relieving motions and consequently flexured fatigue failures are eliminated. Furthermore, the wrap-around concept will effectively eliminate stress concentrations from the top surface contact, as shown below.

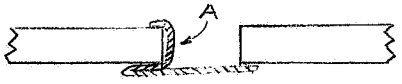

Obviously region A will not be subjected to stress with respect to the solar cell motion.

However, since direct strain will be expected on the interconnector where it bridges the gap between cells, it is necessary to design a system which can handle these strains. Additionally it is desirable to avoid stress concentrations at the electrical bond joints. The wrap-around system definitely avoids stressing the cell's top contact with array motion. However this top contact interconnector must somehow reverse its direction and attach series fashion to the next cell, either through an actual 180° bend or by bonding to a straight conducting strip which connects the cells. The most promising concept would appear to be this latter type. In this way a laminated or vacuum deposited thin film conductor can be made a part of the substrate. Then the wrap-around and bottom (P surface) contact can be made to the pre-etched or deposited circuit. Since the conductor is now a part of the substrate stresses should uniformly distribute themselves along the interconnector and total substrate without concentrating at the bond locations. This can potentially eliminate interconnector flexing and

minimize stress concentrations. This will also allow the use of thinner interconnectors as a means of reducing the interconnector stress and allowing the substrate to carry the load. As shown earlier the stresses on the interconnector were highly dependent upon the interconnector thickness. The standard stress relieved interconnectors analyzed above, utilized thicknesses on the order of one or two mils. The laminated or deposited thicknesses can be 0.5 mils or less. From a conductivity standpoint a 3 micron silver conductor would be sufficient. This therefore, allows a great deal of freedom in the interconnector design. Although it might also be possible to apply a laminate concept to the standard stress relieved interconnector to attain higher fatigue strength with smaller stress loops, the advantages of having the ability for the laminates to distribute stresses, and being easier to handle indicates that there will still probably be a distinct advantage in using the wrap-around technique. With the guidelines sketched above a basis for a series of interconnector concept tests now exists.

One other major design problem does exist with all the above concepts. This is the thermal problem inherent when dissimilar materials are bonded together which have dissimilar coefficients of thermal expansion. The bond point at the solar cell obviously dictates a requirement for matching the coefficients of the interconnectors and solder (if used) to the cell.

The problem of matching to the substrate expansion coefficient is a minor problem since laminates, adhesives, and deposits will not be concentrating stresses in a small region. In fact with aluminum and polyimide, the proximity of coefficients indicates that stresses can reasonably be ignored between these two materials. Practically speaking, since the coefficient of thermal expansion for silicon is so much lower than the majority of interconnector materials presently available this area of concern can be expected to require a significant design effort.

Of interest, there exists a possibility of mixing interconnector materials which are vacuum deposited on a thin substrate so as to effectively provide a connector with a graduated coefficient of thermal expansion from the top surface to the bottom surface. (This will spread thermal stresses throughout the bond region, rather than concentrating them at the interface.) This could in turn be welded or soldered to the solar cell and provide a minimumly stressed contact region. Schematically this is shown below:

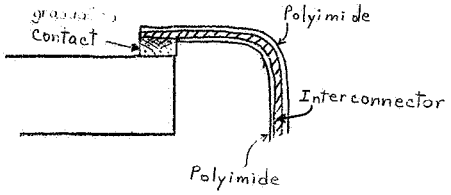

This concept presently appears to be beyond the scope of this program, although these new interconnect designs will open up new areas of study that may provide improvements for future efforts. The present program will be directed toward straight forward thin film metallic interconnector design deposited or laminated onto a flexible substrate material such as a polyimide which will be utilizied in the wrap-around interconnect configuration.

2.4 SUBSTRATE AND SOLAR CELL BONDING SYSTEMS

The substrate for an integrated flexible solar cell array must fulfill a multitude of purposes. Of primary concern, the flexible substrate in contrast to the rigid substrate, which achieves a minimum weight of about 0.200 lb/ft^2, must have a weight less than 0.015 lb/ft^2 including cell bonding adhesive to achieve a power to weight ratio of 100 watts per pound for an array. The array in this study includes the cells, covers, interconnects, adhesives, substrates, and the bus connectors, but does not include the deployment mechanism.

Additional functions of the array substrate which are important are:

1. Maintain solar cell series and parallel spacing
2. Transmit loads from support structure to cell matrix during extension and retraction.
3. Insulate the power transmission bus from the cell matrix
4. Resist UV and hard particle radiation
5. High temperature and vacuum stability
6. Resist flexural fatigue
7. Flexible over a wide temperature range
8. The ability to be bonded using conventional adhesives
9. A reasonable absorptivity to emissivity ratio to insure adequate temperature control unless an additional surface treatment is used.

Although the aforementioned qualities must be considered in designing solar cell arrays in general, this study will direct its attention to the specific properties that are critical to the design of an ultra lightweight flexible array. As the first part of this analysis instead of using a continuous substrate sheet, a polyimide film ribbon of some predetermined width will be investigated as the support for the solar cell matrix. The big advantage of this type substrate design is that it provides support with the least weight and it provides support at the cell edges where it is needed to prevent "flapping" during vibrations and roll up. It also meets all the other functions required

above. The adhesive and primer that were selected for the ribbon experiments are RTV 3145 and Dow Corning 90-198 primer. This adhesive and primer were selected based on the results of tests on a lightweight array study performed by Ryan Aeronautical and Spectrolab.

An analysis to determine the minimum ribbon width was begun by comparing the spring rates of a lap joint in which a strip of 1 mil thick polyimide film was bonded to a solderless solar cell using a thickness of 1.5 mils of RTV 3145 with the 90-198 primer applied to the cell only.

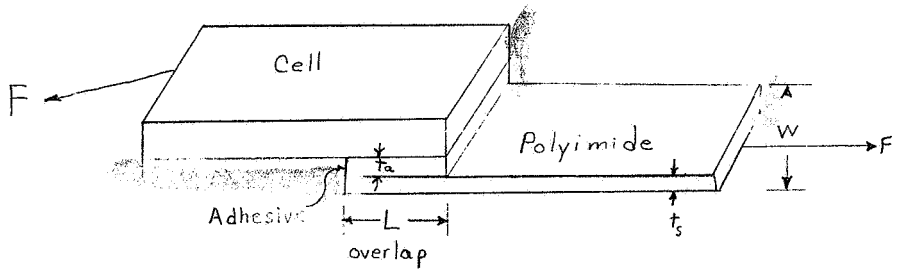

If we consider the above diagram and assume that the lap joint was made using two rigid materials, top and bottom, with an adhesive between, then the spring rates of the rigid members would be high and the joint would transmit stresses uniformly across the adhesive region L . Failure would occur as a straightforward shear failure as determined by the shear modulus of the adhesive material.

In the flexible array case the two members bonded together are not both rigid. Instead, the polyimide has a spring rate that is low. Therefore, when stressed in shear by tensile loading, they develop a nonuniform stress pattern along the lap as shown below.

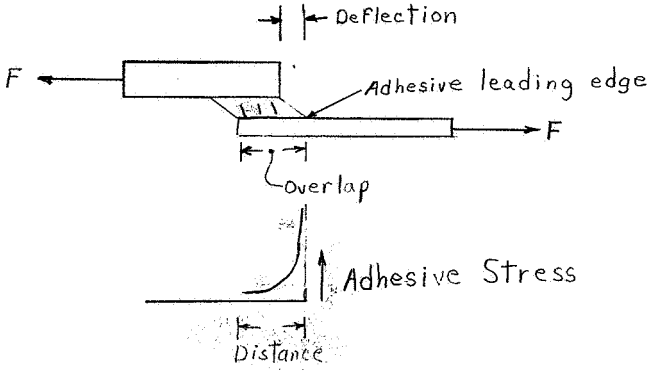

The stress diagram indicates that the peak stress and the failure front will occur at the leading edge of the adhesive and will gradually shift as the tensile load exceeds the bond strength at the adhesive film interface. This failure mechanism will therefore be dependent upon the glue line width W and thickness rather than the overlap length L.

To substantiate this model with experimental data, three-cell series modules were bonded together using polyimide film bonded to the cells with RTV 90-024 (a refined version of RTV 3145) and DC 90-198 primer. Ribbons of 1 mil polyimide film were bonded to the cell rear surface in cell overlap widths of 0.050, 0.100, 0.150, 0.200 and 0.250. The adhesive thickness was about 0.0015 inches in thickness. No interconnects were used in these assemblies. Ten sample modules of each of the five ribbon widths were made and tested. Two mil thick polyimide films were bonded to the ends of the module to provide grips that were stronger than the test joints. The assemblies were subjected to tensile loads until separation occurred. These forces were recorded and the results are presented in Table 2. These data illustrate the lack of dependence of overlap length to failure loads although the 0.050 inch ribbon case starts to indicate a limiting effect. The curve also shows that the fracture in some cases was a cement bond failure C and in other cases a polyimide substrate tear K . The failures were distributed about half-and-half between the two failure modes indicating the system was capable of being stressed to a point near the strength of the substrate material.

Structural loads generated in a large area array during extension and retraction are expected to be on the order of five to ten pounds across a typical array which would be three feet wide or more. The single cell values plotted on Table 2 would therefore indicate that the ribbon substrate system under consideration will be more than adequate for loads anticipated on this design concept.

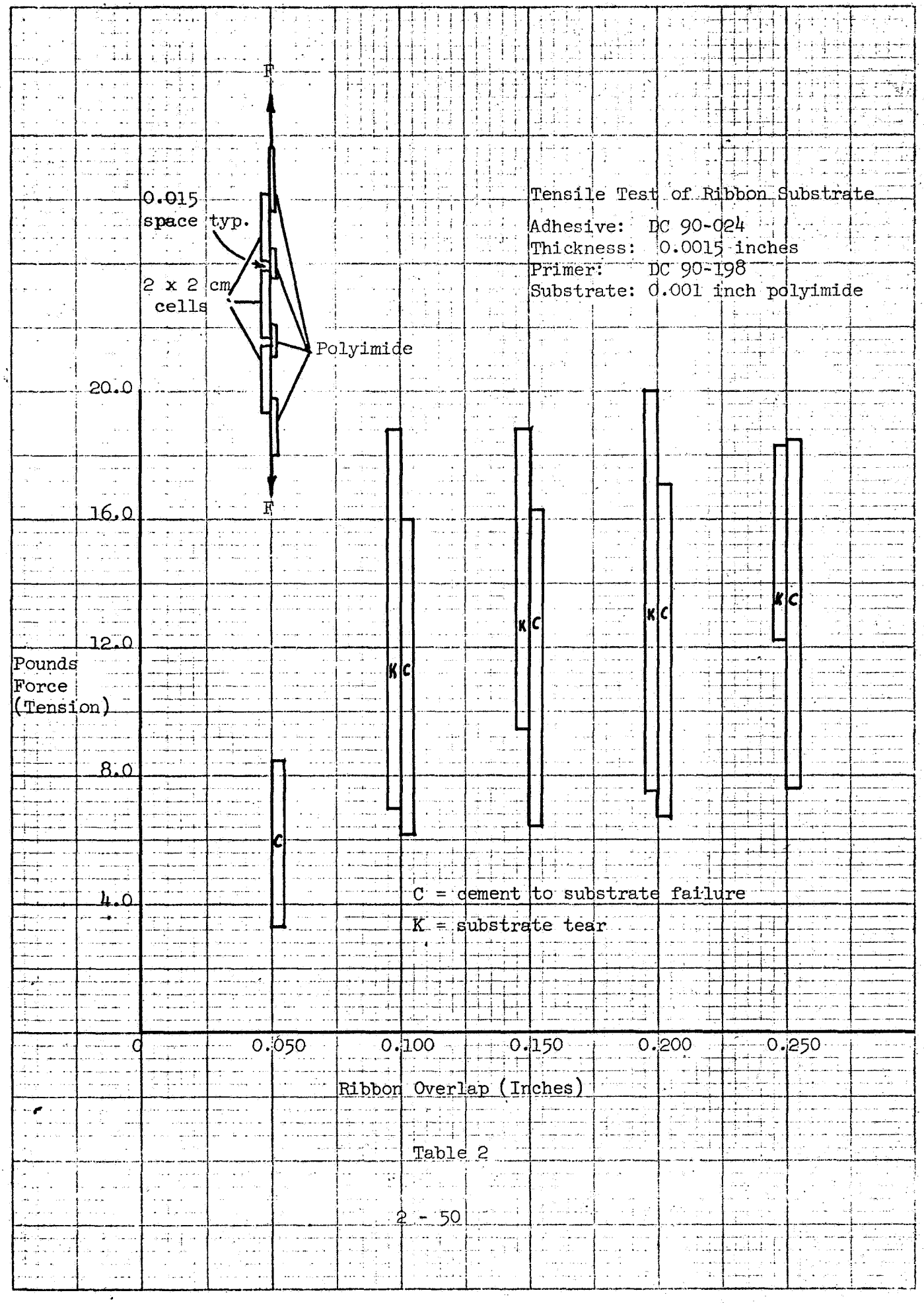
F
0.015 space typ.
2 x 2 cm cells
Polyimide
F
Tensile Test of Ribbon Substrate
Adhesive: DC 90-024
Thickness: 0.0015 inches
Primer: DC 90-198
Substrate: 0.001 inch polyimide
20.0
16.0
12.0
8.0
4.0
0
Pounds Force (Tension)
K C
K C
K C
K C
C
C = cement to substrate failure
K = substrate tear
0.050
0.100
0.150
0.200
0.250
Ribbon Overlap (Inches)

Table 2

3.0 CONCLUSIONS

1) Solar cell cost data indicates that the cost effectiveness can be optimized in 1969 by using an 8 mil thick cell and in 1975 by using a 4 mil thick cell.
2) A ribbon glass cover can be applied with a conventional adhesive in a manner that is adaptable to automation.
3) An inexpensive glass sizing technique which is adaptable to automation has been developed.
4) The stress loop type of interconnector is marginal for fatigue resistance on a flexible solar array.
5) A generalized stress fatigue design equation for interconnectors was developed.
6) A wrap-around concept interconnect appears more suitable for flexible arrays to solve fatigue problems.
7) A ribbon substrate analysis showed that a continuous substrate is not needed and that a ribbon substrate is not limited in strength by overlap until an overlap width of less than 0.100 inches is reached. This allows a much lighter substrate to be used.

4.0 RECOMMENDATIONS

Not applicable.

5.0 REFERENCES

Not applicable.